Photosynthesis Research **46**: 177–184, 1995.

Regular paper

A hydrogen-atom abstraction model for the function of Y_Z in photosynthetic oxygen evolution

Curtis W. Hoganson[1], Nikos Lydakis-Simantiris[1,4], Xiao-Song Tang[2], Cecilia Tommos[3], Kurt Warncke[1], Gerald T. Babcock[1], Bruce A. Diner[2], John McCracken[1] & Stenbjörn Styring[3]

[1]*Department of Chemistry, Michigan State University, East Lansing, MI 48824, USA;* [2]*Central Research and Development Department, Experimental Station, E.I. DuPont de Nemours and Company, Wilmington, Delaware 19880-0173, USA;* [3]*Department of Biochemistry, Arrhenius Laboratories for Natural Sciences, Stockholm University, S-10691 Stockholm, Sweden;* [4]*Department of Chemistry, University of Crete, Iraklion, P.O. Box 1470, Crete, 71409, Greece*

Received 20 March 1995; accepted in revised form 25 May 1995

Key words: electron paramagnetic resonance, manganese cluster, oxygen evolution, oxygen evolving complex, Photosystem II, proton transfer, tyrosine radical, water oxidation

Abstract

Recent magnetic-resonance work on $Y_{\dot{Z}}$ suggests that this species exhibits considerable motional flexibility in its functional site and that its phenol oxygen is not involved in a well-ordered hydrogen-bond interaction (Tang et al., submitted; Tommos et al., in press). Both of these observations are inconsistent with a simple electron-transfer function for this radical in photosynthetic water oxidation. By considering the roles of catalytically active amino acid radicals in other enzymes and recent data on the water-oxidation process in Photosystem II, we rationalize these observations by suggesting that $Y_{\dot{Z}}$ functions to abstract hydrogen atoms from aquo- and hydroxy-bound manganese ions in the $(Mn)_4$ cluster on each S-state transition. The hydrogen-atom abstraction process may occur either by sequential or concerted kinetic pathways. Within this model, the $(Mn)_4/Y_Z$ center forms a single catalytic center that comprises the Oxygen Evolving Complex in Photosystem II.

Introduction

Amino acid side chain radicals have been shown to play essential functional roles in a number of enzyme systems (see Sigel and Sigel 1994 for reviews). In general, these species appear to operate as either hydrogen-atom abstractors or as electron-transfer cofactors. The tyrosyl species in Photosystem II, Y_Z and Y_D, are representative of this class of radical cofactor. Although they occur at symmetry related positions in the D1 and D2 polypeptides that form the core of Photosystem II (Debus et al. 1988; Vermaas et al. 1988; Koulougliotis et al. 1995), they are differentiated sharply, in terms of function (Barry 1993; Hoganson and Babcock 1994; Diner and Babcock 1995). Y_Z operates in a linear sequence to interface the photochemistry that occurs at P680 with the multi-electron, water-splitting chemistry in which the $(Mn)_4$ cluster participates. Y_D, on the other hand, undergoes redox chemistry but is not involved in the catalytic events associated with water oxidation.

Here, we present magnetic resonance data on $Y_{\dot{Z}}$ that provide insight into its dynamics and local protein environment and supplement detailed investigations of the radical that have been reported elsewhere (Tang et al. 1995; Tommos et al. 1995). These observations are compared to and contrasted with analogous data in the literature for and $Y_{\dot{D}}$ for other tyrosyl radicals (Bender et al. 1989; Hoganson and Babcock 1992; Tang et al. 1993; Tommos et al. 1993; Mino and Kawamori 1994; Rigby et al. 1994; Warncke et al. 1994; Tang et al. 1995). The comparison shows that pronounced distinctions occur in both hydrogen bonding and phenol head group motion in this class of radicals that can be correlated with function. $Y_{\dot{Z}}$ and $Y_{\dot{D}}$ can be distinguished on this basis, from which we conclude

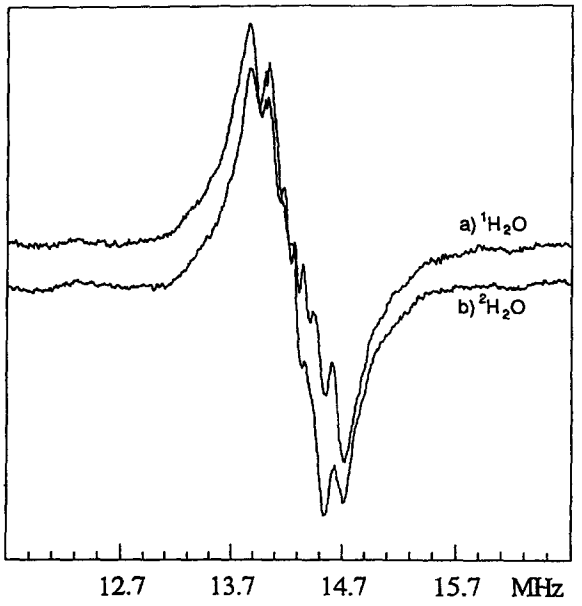

Fig. 1. ENDOR spectra of $Y_{\dot{Z}}$ in the Y_D-less mutant of *Synechocystis* in (a) ^1H_2O or (b) ^2H_2O. Both spectra are in derivative mode and were detected by continuous-wave techniques. The microwave frequency was 9.399 GHz, the magnetic field was 0.3305 T, the microwave power was 2.0 mW, the radiofrequency power was 150 Wat 15 MHz, frequency modulation was 50 kHz, time constant was 0.2 s, the temperature was 110 K, and the proton Larmor frequency was 14.3 MHz.

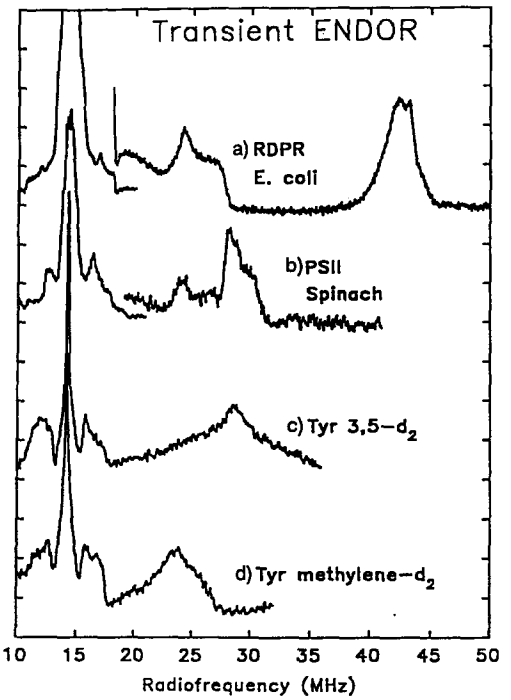

Fig. 2. ENDOR spectra of tyrosyl radicals. All spectra are in absorption mode and were obtained using the transient ENDOR detection scheme (Hoganson and Babcock 1995). (a) Ribonucleotide diphosphate reductase, *E. coli*, 12 K; (b) Photosystem II Y_D, spinach, 12 K; (c) ring 3,5-deuterated tyrosine in $^2H_2O/NaO^2H$ glass, 121 K; (d) methylene-deuterated tyrosine in $^2H_2O/NaO^2H$ glass, 121 K. The radicals in spectra c and d were generated by UV illumination.

that, while Y_D appears tailored to a pure electron-transfer function, Y_Z has characteristics expected of a hydrogen-atom abstractor. This conclusion is combined with those from recent work from other laboratories on $(Mn)_4/Y_{\dot{Z}}$ distance estimates, Photosystem II proton release, and directed mutagenesis to generate a $Y_{\dot{Z}}$ hydrogen-atom abstraction model for water oxidation.

Materials and methods

The procedures for model tyrosyl radical generation, spinach and Synechocystis Photosystem II isolation, $Y_{\dot{Z}}$ trapping, and $^1H_2O/^2H_2O$ exchange follow those described elsewhere (Hoganson and Babcock 1992; Tang et al. 1995; Tommos et al. 1995). The transient ENDOR methodology is described in detail by Hoganson and Babcock (1995) and the electron spin echo envelope modulation (ESEEM) techniques used here are analogous to those used in a recent study of $Y_{\dot{D}}$ in *Synechocystis* by Warncke et al. (1994).

Results

Figure 1 shows continuous-wave ENDOR spectra for $Y_{\dot{Z}}$ trapped in PS II particles from a $Y_{\dot{D}}$-less mutant of *Synechocystis* 6803. In the upper trace, the particles were suspended in an ^1H_2O-containing buffer; in the lower trace, ^1H_2O has been exchanged for ^2H_2O. There are significant changes in the $Y_{\dot{Z}}$ spectrum in the close-coupling region ($\pm$ 1 MHz) around the ^1H Larmor frequency (ν_{1H} = 14.3 MHz for the spectra in Fig. 1) upon solvent isotope exchange, which demonstrates that the $Y_{\dot{Z}}$ site and its close environment (< 5 Å) are accessible to solvent and contain exchangeable protons (see also, Tang et al. 1995). In contrast, we have observed no discernible differences in the spectra beyond those in the matrix region, consistent with both ENDOR (Tang et al. 1995; Tommos et al. 1995) and FTIR (Bernard et al. 1995) data that have been interpreted to indicate the absence of a well-ordered hydrogen bond to the phenol oxygen. The hydrogen-bond status of $Y_{\dot{Z}}$ clearly differs from that of $Y_{\dot{D}}$, for which

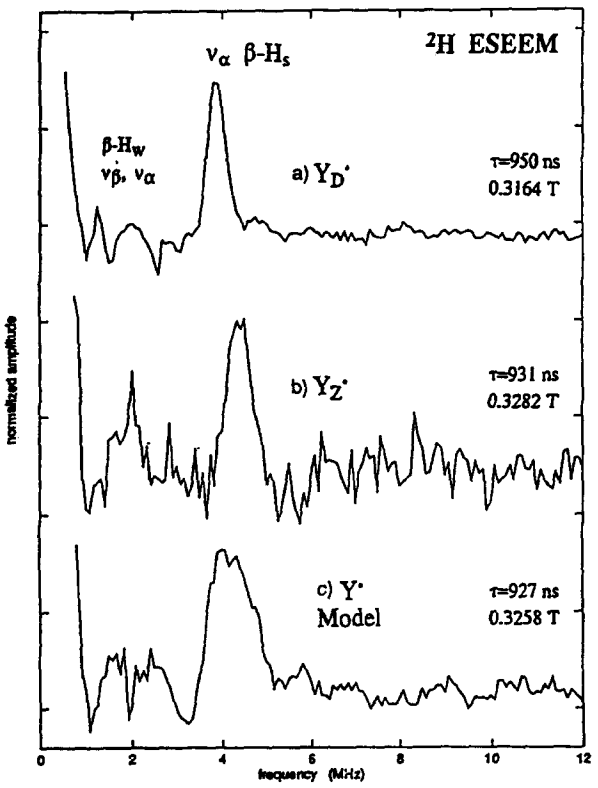

Fig. 3. ^{2}H-ESEEM spectra of (a) $Y_{\dot{D}}$, b) $Y_{\dot{Z}}$, and (c) a model tyrosyl radical in a glass. The Y_D and Y_Z radicals were in *Synechocystis* PS II preparations. Typical spectrometer conditions were microwave frequency = 9.190 GHz, magnetic field = 0.3282 T, τ = 931 ns, (τ + T_0) = 140 ns, microwave pulse power = 40 W (20 ns in duration at full-width, half maximum), pulse sequence repetition rate = 10 Hz, and T = 4K. At this field, ν_{2_H} = 2.1 MHz.

a variety of techniques have shown the occurrence of an exchangeable proton at a distance consistent with its forming a hydrogen bond to the $Y_{\dot{D}}$ phenol oxygen (reviewed in Barry 1993; Hoganson and Babcock 1994).

A further difference between the two tyrosyls in Photosystem II is illustrated by the magnetic-resonance spectra in Figs. 2 and 3. Figure 2 shows transient ENDOR spectra of the $Y_{1\dot{2}2}$ radical in ribonucleotide reductase (Fig. 2a), of $Y_{\dot{D}}$ (Fig. 2b), and of a model tyrosine radical specifically deuterated either at the 3,5 positions (Fig. 2c) or at the b-methylene positions (Fig. 2d). (In the ring-numbering system used here, the 3,5-ring carbons are *ortho* to the phenol oxygen and ring C_1 is bonded to the β-methylene carbon.) The spectra of the specifically labeled model radical confirm the 3,5-^{1}H origin of the features in the 20–26 MHz region. In Figs. 2a–c, the highest frequency resonances arise from the more strongly coupled of the two β-methylene ^{1}H (Hoganson and Babcock 1994). In the transient ENDOR spectra, however, the spectral characteristics of these β-^{1}H resonances are markedly different for the three radicals. For $Y_{1\dot{2}2}$ in RDPR and for $Y_{\dot{D}}$ in Photosystem II, this ^{1}H contributes sharp, well-resolved features at 40–45 MHz and from 27–31 MHz, respectively, reflecting the difference in β-methylene geometry for these two radicals. For the strongly coupled β-^{1}H in the model, qualitatively different behavior is observed as its resonance is spread over 15 MHz with a single maximum at ~ 29 MHz.

Warncke and McCracken (1995) have explored the basis for this difference in resonant behavior for β-^{1}H in tyrosyl radicals by spin echo methods and have shown that rotational mobility about the C_β–C_1 bond can occur to produce a dispersion in β-methylene ^{1}H dihedral angle (θ). Briefly, as the rotational barrier around C_β–C_1 decreases, the phenol head group samples an increasing range of dihedral angle; as the temperature is lowered for magnetic-resonance work, this distribution in θ is frozen in. Because the β-^{1}H hyperfine couplings ($A_{1_{H\beta}}$) are related to dihedral angle according to

$$A_{1_{H\beta}} = B_2 \rho_{c_1} \cos^2 \theta$$

where B_2 is a constant = 162 MHz and ρ_{C_1} is the unpaired electron-spin density at the ring C_1 position, dispersion in θ produces a range of $A_{1_{H\beta}}$ couplings that broadens resonances due to the β-hydrogens. By using ^{2}H ESE techniques and specifically deuterated tyrosyl models, they were able to work out quantitative measures of dihedral angle variation from considerations of β-^{2}H spin-echo lineshape. Figure 3 shows representative deuterium ESEEM spectra for $Y_{\dot{D}}$, $Y_{\dot{Z}}$, and a model tyrosyl radical in which the β-positions in all three radicals have been specially labeled with ^{2}H. In each spectrum, the feature in the 4 MHz region corresponds to the more strongly coupled β-^{2}H (the lower resonant frequency for ^{2}H, relative to ^{1}H, reflects the lower magnetogyric ratio for ^{2}H). The full width at half maximum line widths ($\Delta\nu$) of the β-^{2}H resonance in the three radicals vary significantly, which indicates varying degrees of rotational dispersion. For $Y_{\dot{D}}$, $\Delta\nu$ = 0.48 MHz; for $Y_{\dot{Z}}$, $\Delta\nu$ = 0.71 MHz; and for the model, $\Delta\nu$ = 1.21 MHz. Error estimates based on measuring the β-^{2}H linewidths in these samples at various τ values (at least nine different τ values were used for each

sample) sets the limits of uncertainty in $\Delta\nu$ at $\pm$ 0.03 MHz. Quantitative analysis indicates that θ dispersion increases from $Y_{\dot{D}}$ ($\Delta\theta \pm 4°$), to $Y_{\dot{Z}}$ ($\Delta\theta \sim \pm 7°$), to the model tyrosyl ($\Delta\theta \sim \pm 30°$). For $Y_{\dot{D}}$, the $\pm$ 4° value is an upper limit; the uncertainty in the angular variation for $Y_{\dot{Z}}$ and the model tyrosine is $\pm$ 0.5°. A clear conclusion from this analysis is that there is considerably more rotational mobility in the $Y_{\dot{Z}}$ C_β–C_1 bond than in the analogous bond in $Y_{\dot{D}}$.

Discussion

The results presented above and elsewhere (Mino and Kawamori 1994; Roffey et al. 1994; Bernard et al. 1995; Tang et al. 1995; Tommos et al. 1995) indicate that there are surprising differences between $Y_{\dot{D}}$ and $Y_{\dot{Z}}$, in terms of their hydrogen bonding and dynamic behavior. The phenol head group of $Y_{\dot{D}}$ is rigid and essentially immobilized in a homogeneous conformation about the C_β–C_1 bond; its phenol oxygen is involved in a well-defined hydrogen-bond interaction with a nearby residue, most likely H-189 of the D2 polypeptide (Tang et al. 1993; Tommos et al. 1993). These observations, together with the likelihood that $Y_{\dot{D}}$ occurs in a hydrophobic environment (Svensson et al. 1991; Hoganson and Babcock 1994), are consistent with what would be expected for a pure electron-transfer cofactor – nuclear motion along the electron-transfer reaction coordinate is suppressed so that the reorganization energy (λ) is minimized. Small λ values maximize the rate of the electron-transfer process at a given driving force. This principle is clearly apparent in other pure electron-transfer cofactors such as the blue copper proteins and the cytochromes *b* and *c* (see Williams (1990) for a review). Thus, the 'proton rocking' model for the redox chemistry associated with $Y_{\dot{D}}$ (Scheme 1),

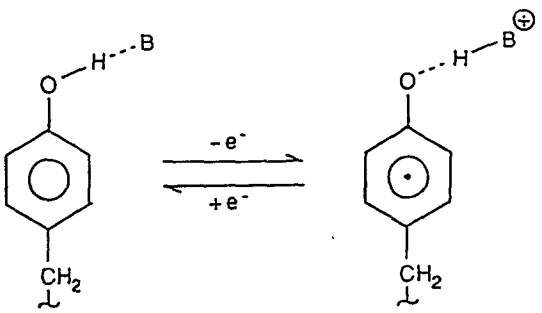

Scheme 1

is consistent with both structural and functional properties of $Y_{\dot{D}}$ (Babcock et al. 1989). The phenol proton of Y_D is hydrogen bonded to a nearby basic residue (H189(D2)); upon oxidation, the proton is retained in the site, the sense of the hydrogen-bond interaction is reversed, and nuclear motion is minimized.

At the outset, we expected to see similar design principles implemented for Y_Z, as the conventional view of Photosystem II envisions this species as playing a pure electron-transfer role to effect rapid, quantum yield-preserving reduction of $P680^+$ and subsequent oxidation of the $(Mn)_4$ cluster. The results discussed here, however, show that this is not the case, which suggests that reconsideration of the conventional view of Y_Z function is necessary.

Several pieces of data relevant to such a reconsideration are available from other labs. Savéant (1993), in electrochemical work, has shown that phenol oxidation involves H-atom transfer, that is, concerted hydrogen ion and electron motion. We expect that this principle will be in force for Y_Z and that its oxidation will be coupled to its deprotonation. The results here, as well as those reported elsewhere (Bernard et al. 1995; Tang et al. 1995; Tommos et al. 1995), indicate that $Y_{\dot{Z}}$ is unlikely to be involved in a well-defined hydrogen-bond interaction, which suggests that the proton leaves the Y_Z site upon oxidation. One view of proton release during water-oxidation is consistent with this; each S-state transition is accompanied by stoichiometric proton release (Lübbers et al. 1993). This phenomenon is obscured, in thylakoids and Photosystem II membranes, by the buffering action of amino acid side chains but is clearly observed in Photosystem II core preparations. Moreover, Haumann and Junge (1994) have shown that this proton release is coupled to the oxidation of Y_Z, not its reduction, in agreement with the considerations above. It has been shown, however, that H190(D1) is essential in promoting rapid reduction of $P680^+$ by Y_Z, as mutagenesis of this species slows the rate of the Y_Z $P680^+$ reaction by a factor of 200 (Diner et al. 1991; Tang et al. 1993; Kramer et al. 1994; Roffey et al. 1994). These observations suggest that H190(D1) plays an essential role in facilitating the concerted hydrogen-atom (i.e. coupled proton/electron) transfer that occurs upon Y_Z oxidation by functioning as an immediate, but transient, proton acceptor. Mutagenesis of this species, to remove its base function, would be expected to slow electron transfer by impeding the coupled proton release; in effect, the transient $Y_{\dot{Z}}/Y_Z$ redox potential would

increase. Taken together, these considerations suggest a 'proton sloughing' set of reactions upon Y_Z oxidation, as summarized in Scheme 2:

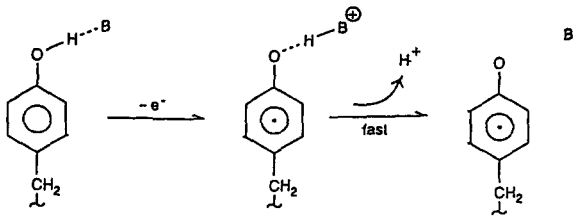

Scheme 2

In this sequence, we hypothesize that B represents H190(D1). The first step in the sequence represents concerted H-atom transfer, as oxidation and formation of the H–B bond are viewed as occurring simultaneously. In the second step, proton release from the site occurs on the μs time scale (Haumann and Junge 1994). We stress that the proton release in the second step is not viewed as occurring directly to bulk phase. Rather, we suggest that it occurs to other protein acid/base groups, which will, depending on the solution pH and intactness of the preparation, eventually deprotonate in a complex fashion to bulk phase (Lavergne and Junge 1993). The Y_Z environment is likely to be more hydrophilic than that of Y_D, as indicated by the occurrence of conserved carboxylic acid residues in D1 that do not occur in D2 (Svensson et al. 1990, 1991). These side chains may serve as secondary proton acceptors and provide the deprotonation pathway implied in the second step above that would facilitate proton efflux from the Y_Z site; conversely, their absence in D2 would confine the proton to the Y_D site, as indicated in Scheme 1.

Scheme 2 indicates that the Y_Z site sloughs its proton upon oxidation; the postulated hydrogen-bonding interaction with H190(D1) lowers the redox potential of Y_Z and minimizes λ, thus preserving the high rate of electron transfer to $P680^+$. At the conclusion of this process, a tyrosyl radical, unencumbered by hydrogen bonds and with a good deal of motional lability, remains. A likely function for this radical in water oxidation is suggested by several bits of information. Inspection of the functional amino acid radical literature (Frey 1990; Sigel and Sigel 1994) indicates that the underlying catalytic role of these radical species involves hydrogen-atom abstraction from substrate. An oxygen-activating metal center serves to produce the radical by using the water/oxygen couple as an electron sink. A generalized mechanism for this sequence of events is summarized in Scheme 3:

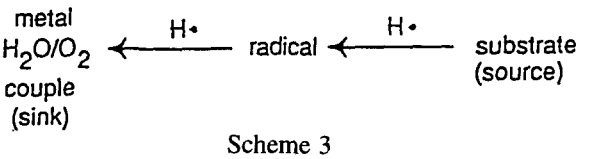

Scheme 3

Moreover, in those enzymes for which crystal structures are available (e.g. prostaglandin synthase, Picot et al. 1994), the oxygen-activating metal center is in close physical proximity (< 10 Å) to the redox active amino acid.

These insights carry over to Photosystem II in two contexts. First, the original EPR work on $S_nY_{\dot{Z}}$ reaction kinetics showed that the $S_3Y_{\dot{Z}}$ reaction rate-limited the water-oxidation chemistry, i.e., that O=O bond formation and dioxygen release were fast, compared to the reduction of $Y_{\dot{Z}}$ by S^3 (Babcock et al. 1976). This suggests that significant nuclear rearrangements occur upon the rereduction of $Y_{\dot{Z}}$ and that these raise λ sufficiently to manifest themselves by rate limiting the chemistry. The absence of a hydrogen bond to $Y_{\dot{Z}}$ implicates protonic motion as the source of the nuclear rearrangement. Second, Britt and co-workers have shown that the source of the split S_3 signal in Ca^{2+}-depleted Photosystem II preparations is a tyrosyl radical involved in a magnetic interaction with the manganese cluster (Gilchrist Jr. et al. 1995). By assuming that the interaction is dipolar, they were able to estimate a distance of ~ 4.5 Å between the two paramagnets. A comparison of the details of the spectrum of the tyrosyl radical in the split S_3 species, which shows significantly broadened β-^{1}H resonances relative to those for Y_D in the same sample, with that of $Y_{\dot{Z}}$ that we report here and elsewhere (Tommos et al. 1995) indicates similar motional lability, which provides support for the identification of the split S_3 tyrosyl with $Y_{\dot{Z}}$.

Taken together, these results suggest that strong analogies exist between $Y_{\dot{Z}}$ in Photosystem II and the other radical enzymes that have been studied. Relative to these other systems, Photosystem II appears simply to reverse the direction of hydrogen-atom flow: a water-activating metal center acts as substrate for a radical center generated by photochemistry at P680. Scheme 4 summarizes the process envisioned, where

the notation "H·" reflects the idea that H· transfer may be either sequential or concerted (see below):

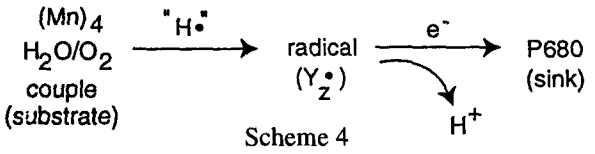

Scheme 4

The motional lability that we have detected and quantified for $Y_{\dot{Z}}$ is essential in this model, as the deprotonation/reprotonation reactions are viewed as directional. Y_Z deprotonates to H190(D1), which is likely to be oriented toward P680, whereas its reprotonation occurs from the H_2O $(Mn)_4$ center, which is likely to be more remote from the reaction center chlorophylls. Thus, in order to assure proper disposition of the phenol head group during the acid/base chemistry, motional flexibility is necessary. These geometric considerations are likely to be especially critical, in view of the short deBroglie wavelength and correspondingly short tunneling distances for hydrogen, relative to electrons, and is, most likely, the underlying physical basis for the theme of close physical proximity between metal and radical centers in radical enzymes.

To complete construction of the model, we suggest that hydrogen-atom abstraction chemistry occurs on each S-state transition, according to Scheme 5.

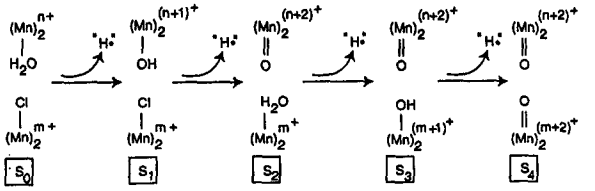

Scheme 5

In this model, the $(Mn)_4$ cluster consists of two magnetically coupled $(Mn)_2$ dimers that serve to anchor and position the substrate and to act as a redox pool to absorb oxidizing equivalents. Accordingly, the hydroxy and oxo ligands to the manganese dimers in the scheme carry formal charges of -1 and -2, respectively. Chloride binds to one of the two dimer halves in the low S-states to block the site and prevent peroxide formation in S_2, which might be likely if two $(Mn)_2$-OH species were allowed to form (Rutherford et al. 1992). Dioxygen formation occurs as two Mn=O species, held in close physical proximity, condense to form the O=O bond in S_4 and leave as dioxygen (see Naruta et al. 1994). The model is satisfying in postulating a critical role for Cl^- in the water-splitting process and in accounting for the recent $^{16}O/^{18}O$ exchange work carried out by Messinger et al. (1995). These authors showed that one of the two oxygens in the S_3 state is only slowly exchangeable, consistent with Scheme 5, as we would expect a difference in exchange kinetics for the bound oxo and hydroxo species depicted in the S_3 state.

The Cl^-/H_2O exchange that occurs on the $S_1 \rightarrow S_2$ transition in Scheme 5 is interesting, as it results in a net positive charge accumulating on the cluster in the S_2 state, which persists to S_3. This behavior is roughly consistent with the long time behavior of the electrochromic shifts that occur upon S-state advance (Rappaport and Lavergne 1991). We realize, however, that chloride involvement is likely to be more complex than that shown in Scheme 5, as Cl^- is clearly involved in the S_2 state under certain conditions (Sandusky and Yocum 1986; Ono et al. 1986). Moreover, whether Scheme 5 can be developed to rationalize the details of both the extent and kinetics of the electrochromic shifts, which appear to correlate well with the net charge change determined by the balance of electrons and protons (Rappaport et al. 1994), remains to be determined.

Essential to the model presented here is the ability of the $Y_{\dot{Z}}$ tyrosyl radical to abstract a hydrogen atom from water or hydroxyl coordinated to the manganese cluster. The kinetic details of the hydrogen-atom abstraction process may involve either concerted H· transfer or sequential H^+, e^- transfer (e.g. Foti et al. 1994); recent isotope effect measurements on the reduction of $Y_{\dot{Z}}$ by the high S states suggest that a process that is more sequential may be favored (Renger et al. 1994; Lydakis-Simantiris and Babcock, unpublished). Regardless of the details of the mechanistic pathway, however, evidence for the lack of a hydrogen bond to $Y_{\dot{Z}}$ and enhanced mobility of the ring around the C_1–C_β axis, which we have obtained experimentally, are consistent with the requirements of the model and with each other. It is necessary to point out, however, several caveats associated with the model presented here. First, the magnetic resonance and FTIR work that has been carried out to suggest motional flexibility and the absence of an exchangeable proton has been done on core complexes lacking the manganese cluster. The work of Britt and co-workers indicates, however, that this mobility is at least conserved in the presence of the cluster under Ca^{2+} depleted conditions. Second, the lack of detection of a well-ordered, exchangeable

proton from the ENDOR of $Y_{\dot{Z}}$ is not absolutely compelling as an argument against hydrogen bonding. Such bonding in a disordered site could produce variations in hydrogen bond length that are not observable in ENDOR or ESE as discrete, well-defined resonances like those of $Y_{\dot{D}}$. However, the requirements of the model could still be met if there were hydrogen bonding to $Y_{\dot{Z}}$, but not in the conformation of the radical that abstracts the hydrogen atom. Moreover, disordered hydrogen bonding, as well as motional lability of $Y_{\dot{Z}}$ and the hydrophilicity of the $Y_{\dot{Z}}$ site, are inconsistent with a simple electron-transfer function for the side chain. Instead, they point to a more complex activity. Finally, the model postulated in Scheme 5 above, while providing a role for Cl^- in water oxidation, is mute on the Ca^{2+} requirement.

Despite these caveats, however, a hydrogen-atom abstraction model accounts well for several critical observations on the water-oxidation process. Moreover, it casts the PS II/OEC complex within the larger class of radical enzymes and provides a useful target for the design of additional experimental inquiries.

Acknowledgements

This work was supported by NIH and USDA grants to GTB, by NRI/CGP/USDA to BAD, by NIH to JMcC, by The Foundation BLANCEFLOR Boncompagni-Ludovisi, née Bildt to CT, and by the Swedish Natural Science Research Council to SS.

References

Babcock GT, Barry BA, Debus RJ, Hoganson CW, Atamian M, McIntosh L, Sithole I and Yocum CF (1989) Water oxidation in Photosystem II: From radical chemistry to multielectron chemistry. Biochemistry 28: 9557–9565

Babcock GT, Blankenship RE and Sauer K (1976) Reaction kinetics for positive charge accumulation on the water side of chloroplast Photosystem II. FEBS Lett 61: 286–289

Barry B (1993) The role of redox active amino acids in the photosynthetic water-oxidizing complex. Photochem Photobiol 57: 179–188

Bender CJ, Sahlin M, Babcock GT, Barry BA, Chandrashekar TK, Salowe SP, Stubbe J, Lindstrom B, Petersson L, Ehrenberg A and Sjoberg B-M (1989) An ENDOR study of the tyrosyl free radical in ribonucleotide reductase from *Escherichia coli*. J Am Chem Soc 111: 8076–8083

Bernard MT, MacDonald GM, Nguyen AP, Debus RJ and Barry BA (submitted) A difference infrared study of hydrogen bonding to the Z· tyrosyl radical of Photosystem II. J Biol Chem

Debus RJ, Barry BA, Babcock GT and McIntosh L (1988) Site-directed mutagenesis identifies a tyrosine radical involved in the photosynthetic oxygen-evolving system. Proc Natl Acad Sci USA 85: 427–430

Diner BA and Babcock GT (in press) Structure, dynamics, and energy conversion efficiency in Photosystem II. In: Ort D and Yocum C (eds) Oxygenic Photosynthesis: The Light Reactions. Kluwer, Dordrecht, The Netherlands

Diner BA, Nixon PJ, and Farchaus JW (1991) Site-directed mutagenesis of photosynthetic reaction centers. Curr Op Struct Biol 1: 546–554

Foti M, Ingold KU and Lusztyk J (1994) The surprisingly high reactivity of phenoxyl radicals. J Am Chem Soc 116: 9440–9447

Frey PA (1990) Importance of organic radicals in enzymatic cleavage of unactivated C-H bonds. Chem Rev 90: 1343–1357

Gilchrist, Jr ML, Ball JA, Randall DW and Britt RD (submitted, 1995) Proximity of the manganese cluster of the photosynthetic oxygen evolving complex to the redox active tyrosine $Y_{\dot{Z}}$. Science

Haumann M and Junge W (1994) Extent and rate of proton release by photosynthetic water oxidation in thylakoids: Electrostatic relaxation versus chemical production. Biochemistry 33: 864–872

Hoganson CW and Babcock GT (1992) Protein-tyrosyl radical interactions in Photosystem II studied by ESR and ENDOR spectroscopy: Comparison with ribonucleotide reductase and in vitro tyrosine. Biochemistry 31: 11874–11880

Hoganson CW and Babcock GT (1994) Photosystem II. In: Sigel H and Sigel A (eds) Metal Ions in Biological Systems, Vol 30, Metalloenzymes Involving Amino Acid-Residue and Related Radicals, pp 77–108. Marcel-Dekker, New York

Hoganson CW and Babcock GT (1995) Detecting the transient ENDOR response. J Mag Res, Series A112: 220–224

Koulougliotis D, Tang X-S, Diner BA and Brudvig GW (1995) Spectroscopic evidence for the symmetric location of tyrosines D and Z in Photosystem II. Biochemistry 34: 2850–2856

Kramer DM, Roffey RA, Govindjee and Sayre RT (1994) The A_T thermoluminescence band from *Chlamydomonas reinhardtii* and the effects of mutagenesis of histidine residues on the donor side of the Photosystem II D1 polypeptide. Biochim Biophys Acta 1185: 228–237

Lavergne J and Junge W (1993) Proton release during the redox cycle of the water oxidase. Photosynth Res 38: 279–296

Lübbers K, Haumann M and Junge W (1993) Photosynthetic water oxidation under flashing light. Oxygen release, proton release and absorption transients in the near ultraviolet – a comparison between thylakoids and a reaction-centre core preparation. Biochim Biophys Acta 1183: 210–214

Messinger J, Badger M and Wydrzynski T (submitted) Detection of *one* slowly exchanging substrate water molecule in the S_3 state of Photosystem II. Proc Natl Acad Sci USA

Mino H and Kawamori A (1994) Microenvironments of tyrosine D^+ and tyrosine Z^+ in Photosystem II studied by proton matrix ENDOR. Biochim Biophys Acta 1185: 213–220

Naruta Y, Sasayama M and Sasaki T (1994) Oxygen evolution by oxidation of water with manganese porphyrin dimers. Angew Chem Int Ed Engl 33: 1839–1841

Ono T, Zimmermann JL, Inoue Y and Rutherford AW (1986) EPR evidence for a modified S-state transition in chloride-depleted Photosystem II. Biochim Biophys Acta 851: 193–201

Picot D, Loll PJ and Garavito RM (1994) The x-ray crystal structure of the membrane protein prostaglandin H2 synthase-1. Nature 367: 243–249

Rappaport F and Lavergne J (1991) Proton release during successive oxidation steps of photosynthetic water oxidation: Stoichiometries and pH dependence. Biochemistry 30: 1004–10012

Rappaport F, Blanchard-Desce M and Lavergne J (1994) Kinetics of electron transfer and electrochromic change during the redox transitions of the photosynthetic oxygen-evolving complex. Biochimica et Biophysica Acta 1184: 178–192

Renger G, Bittner T and Messinger J (1994) Structure-function relationship in photosynthetic water oxidation. Biochem Soc Trans 22: 318–322

Rigby SEJ, Nugent JHA and O'Malley PJ (1994) The dark stable tyrosine radical of Photosystem 2 studied in three species using ENDOR and EPR spectroscopies. Biochemistry 33: 1734–1742

Roffey RA, Van Wijk KJ, Sayre RT, and Styring S (1994) Spectroscopic characterization of Tyrosine-Z in Histidine 190 mutants of the D1 protein in Photosystem II (PS II) in *Clamydomonas rheinhardtii*. J Biol Chem 269: 5115–5121

Rutherford AW, Zimmermann J-L and Boussac A (1992) Oxygen evolution: In: Barber J (ed) The Photosystems: Structure, Function and Molecular Biology, pp 179–229. Elsevier, Amsterdam

Sandusky PO and Yocum CF (1986) The chloride requirement for photosynthetic oxygen evolution: Factors affecting nucleophilic displacement of chloride from the oxygen-evolving complex. Biochim Biophys Acta 849: 85–93

Savéant (1993) Electron transfer, bond breaking, and bond formation. Acc of Chem Res 26(9): 455–461

Sigel H and Sigel A (1994) (eds) Metal Ions in Biological Systems, Metalloenzymes involving amino acid-residue and related radicals, Vol 30. Marcel-Dekker, New York

Svensson B, Vass I, Cedergren E and Styring S (1990) Structure of donor side components in Photosystem II predicted by computer modeling. EMBO J 9: 2051–2059

Svensson B, Vass I and Styring S (1991) Sequence analysis of the D1 and D2 reaction center proteins of Photosystem II. Z Naturforsch 46c: 765–776

Tang X-S, Chisholm DA, Dismukes GC, Brudvig GW, and Diner BA (1993) Spectroscopic evidence from site-directed mutants of *Synechocystis* PCC6803 in favor of a close interaction between Histidine 189 and redox-active Tyrosine 160, both of polypeptide D2 of the Photosystem II reaction center. Biochemistry 32: 13742–13748

Tang XS, Zheng M, Chisholm DA, Dismukes GC and Diner BA (submitted, 1995) Investigation of the differences in the local protein environments surrounding tyrosine radicals, $Y_{\dot{Z}}$ and $Y_{\dot{D}}$, in Photosystem II, using wild-type and the D2-Tyr160Phe mutant of *Synechocystis* 6803. Biochemistry

Tommos C, Davidsson L, Svensson B, Madsen C, Vermaas W and Styring S (1993) Modified EPR spectra of the tyrosine$_D$ radical in Photosystem II in site-directed mutants of *Synechocystis* sp. PCC 6803: Identification of side chains in the immediate vicinity of tyrosine$_D$ on the D2 protein. Biochemistry 32: 5436–5441

Tommos C, Tang X-S, Warncke K, Hoganson CW, Styring S, McCracken J, Diner BA, and Babcock GT (1995) Spin density distribution, conformation, and hydrogen-bonding status of the redox active tyrosine Y_Z from multiple electron magnetic resonance spectroscopies: Implications for photosynthetic oxygen evolution. J Am Chem Soc (in press)

Vermaas WFJ, Rutherford AW and Hansson O (1988) Site-directed mutagenesis in Photosystem II of the cyanobacterium *Synechocystis* sp. PCC 6803: Donor D is a tyrosine residue in the D2 protein. Proc Natl Acad Sci USA 85: 8477–8481

Warncke K and McCracken J (1995) Rotational mobility in tyrosyl radicals. J Chem Phys (in press)

Warncke K, McCracken J, and Babcock GT (1994) Structure of the Y_D tyrosine radical in Photosystem II as revealed by ^2H electron spin echo envelope modulation (ESEEM) spectroscopic analysis of hydrogen hyperfine interactions. J Am Chem Soc 116: 7332–7340

Williams RJP (1990) Overview of biological electron transfer. In: Johnson MK, King BR, Kurtz Jr DM, Kutal C, Norton ML and Scott RA (eds) Electron Transfer in Biology and the Solid State. ACS Advances in Chemistry Series, Vol 226, pp 3–23. American Chemical Society, Washington DC